Tetracaine Reports a Conformational Change in the Pore of Cyclic Nucleotide–gated Channels

ANTHONY A. FODOR, KEVIN D. BLACK, and WILLIAM N. ZAGOTTA

From the Department of Physiology and Biophysics, Howard Hughes Medical Institute, University of Washington School of Medicine, Seattle, Washington 98195-7290

ABSTRACT Local anesthetics are a diverse group of clinically useful compounds that act as pore blockers of both voltage- and cyclic nucleotide–gated (CNG) ion channels. We used the local anesthetic tetracaine to probe the nature of the conformational change that occurs in the pore of CNG channels during the opening allosteric transition. When applied to the intracellular side of wild-type rod CNG channels expressed in *Xenopus* oocytes from the α subunit, the local anesthetic tetracaine exhibits state-dependent block, binding with much higher affinity to closed states than to open states. Here we show that neutralization of a glutamic acid in the conserved *P* region (E363G) eliminated this state dependence of tetracaine block. Tetracaine blocked E363G channels with the same effectiveness at high concentrations of cGMP, when the channel spent more time open, and at low concentrations of cGMP, when the channel spent more time closed. In addition, Ni^{2+}, which promotes the opening allosteric transition, decreased the effectiveness of tetracaine block of wild-type but not E363G channels. Similar results were obtained in a chimeric CNG channel that exhibits a more favorable opening allosteric transition. These results suggest that E363 is accessible to internal tetracaine in the closed but not the open configuration of the pore and that the conformational change that accompanies channel opening includes a change in the conformation or accessibility of E363.

KEY WORDS: local anesthetic • photoreceptor • cyclic GMP

INTRODUCTION

Cyclic nucleotide–gated (CNG)[1] ion channels are key players in visual and olfactory signal transduction pathways (reviewed in Lancet, 1986; Yau and Baylor, 1989; Zufall et al., 1994). Although they are only weakly voltage dependent, CNG channels have regions of sequence similarity with voltage-gated channels (Jan and Jan, 1990). One region of high conservation between CNG channels and voltage-gated channels is the *P* region, thought to line a portion of the ion-conducting pore. *Shaker* K^+ channels that have had portions of their *P* region replaced with the corresponding region from CNG channels take on many of the permeation properties of CNG channels (Heginbotham et al., 1992). These chimeric channels become permeable to Na^+ as well as to K^+ and become blocked by the divalent cations Mg^{2+} and Ca^{2+}.

Like voltage-gated channels, CNG channels are thought to possess multi-ion pores (Furman and Tanaka, 1990; Sesti et al., 1995). The external divalent cation binding site is thought to involve the E363 position in the *P* region of CNG channels (Root and MacKinnon, 1993; Eismann et al., 1994). Neutralization of this binding site eliminates anomalous mole-fraction dependence (Sesti et al., 1995) and external block by protons (Root and MacKinnon, 1994) and divalent cations (Root and MacKinnon, 1993; Eismann et al., 1994) while still leaving the channels vulnerable to internal block by divalent cations. This suggests that there is a second, internal cation binding site. The specific residues that contribute to this internal binding site remain unknown.

Another feature in common between voltage-gated channels and CNG channels is block by local anesthetics. Local anesthetics are a family of chemically related compounds that have a bulky, hydrophobic end that makes them lipid soluble and a tertiary amine group that, in most local anesthetics, is positively charged at pH 7. Local anesthetics are state-dependent blockers that appear to bind preferentially to the inactivated state of voltage-gated sodium channels (Hille, 1992).

The local anesthetic tetracaine has recently been shown to produce a state-dependent block of rod and olfactory CNG channels (Fodor et al., 1997). Tetracaine becomes more effective at blocking CNG channels under conditions that permit the channels to spend more time in closed states, such as low concentrations of cGMP or saturating concentrations of cAMP. At saturating concentrations of cGMP, the rod CNG channel spends more time in closed states than does the olfactory CNG channel (Goulding et al., 1994; Gordon and Zagotta, 1995*b*). Under these conditions, tetracaine is

Address correspondence to William N. Zagotta, Department of Physiology and Biophysics, Howard Hughes Medical Institute, University of Washington School of Medicine, Box 357290, Seattle, WA 98195-7290. Fax: 206-543-0934; E-mail: zagotta@u.washington.edu

[1]*Abbreviation used in this paper:* CNG, cyclic nucleotide–gated.

more effective at blocking the rod channel than the olfactory channel. These results suggest that tetracaine binds to closed states of CNG channels with approximately three orders of magnitude higher affinity than to open states. In addition, tetracaine block is voltage dependent, becoming more effective at depolarized voltages. The voltage dependence of tetracaine is similar to the voltage dependence observed in the related compounds amiloride and l-*cis*-diltiazem (Haynes, 1992; McLatchie and Matthews, 1992; McLatchie and Matthews, 1994). This voltage dependence is consistent with the hypothesis that tetracaine blocks the pore of CNG channels. The existence of a state-dependent pore block suggests that the inner mouth of the pore of CNG channels undergoes a conformational change during channel opening. In this paper, we find that a mutation of the E363 residue within the *P* region disrupted tetracaine's high affinity binding to the closed state. This suggests that the conformational change within the pore during channel opening involves movement of the E363 residue.

METHODS

The methods in this paper follow those previously described (Fodor et al., 1997). Briefly, the cDNA clone for the α subunit (subunit 1) of the bovine rod channel was isolated, and the amino acid sequence was identical to the published sequence (Kaupp et al., 1989). Site-directed mutations were generated using a technique based on PCR. Oligonucleotide primers were synthesized with the appropriate point mutations and were used to generate insert fragments by PCR. The mutant inserts were ligated in place of the corresponding regions of the wild-type channel. Verification of the mutations was confirmed by DNA sequencing. The splice site of the amino terminal chimera CHM15 was located at residue T162 in the rod channel or W141 in the olfactory channel.

Channel expression and electrophysiological recordings were as previously described (Fodor et al., 1997). Briefly, *Xenopus* oocytes were injected with cRNA coding for the appropriate channel, incubated for 3–10 d at 16°C, and patch-clamped in the inside-out configuration using ~500 KΩ borosilicate pipettes. Solution changes to the cytoplasmic side of the patch were made with an RSC100 rapid solution changer (Molecular Kinetics, Pullman, WA). Tetracaine and cyclic nucleotides were obtained from Sigma Chemical Co. (St. Louis, MO). Tetracaine and cGMP were added to a low divalent NaCl solution that contained 130 mM NaCl, 3 mM HEPES, and 200 μM EDTA. All solutions were adjusted to pH 7.2 with NaOH. The pipette solution consisted of the low divalent NaCl solution without added tetracaine or cyclic nucleotides. The leak currents in the absence of cyclic nucleotides at the corresponding voltages were subtracted from each record. All experiments were performed at room temperature (~20°C). Currents were filtered at 2 KHz and sampled at 20 KHz. Data analysis was performed with the graphical analytical software Igor (WaveMetrics, Lake Oswego, OR). Fits to the model in the text were generated as previously described (Fodor et al., 1997).

In the absence of tetracaine, the currents at depolarized voltages exhibited a small sag due to ion accumulation or depletion as indicated by the small tail currents seen when stepping back to 0 mV (Zimmerman et al., 1988). The sag in current was generally <10%. The error caused by ion accumulation was therefore ignored, and all currents were measured at the end of the voltage pulse to allow channel gating and tetracaine block to reach steady state.

Upon excision, currents recorded from the E363G mutation tended to "run up" slowly with a time course of ~10–20 min. Experiments performed with E363G mutants, therefore, were performed approximately one half hour after the patch had been excised. During this time, currents in the presence of 2 mM cGMP were measured with a pulse to +60 mV every 10 s. Experiments were performed only when the currents measured by these pulses did not change over a period of several minutes. At the end of the experiments, currents in both mutant and wild-type channels were again checked in the presence of 2 mM cGMP and the data were not used if the current had changed by >~25%.

RESULTS

The E363G mutation eliminated the cGMP dependence of tetracaine block. cRNA coding for the α subunit of the rod CNG channel was injected into *Xenopus* oocytes, from which inside-out excised patch-clamp recordings were obtained. Fig. 1 *A* shows recordings made with voltage steps from 0 to +60 mV from a patch containing wild-type rod channels in the presence of either 2 mM or 32 μM cGMP. The top trace in each panel shows the current in the absence of tetracaine and the bottom trace in each panel shows the current in the presence of 10 μM tetracaine. For wild-type channels, 10 μM tetracaine blocked 70.6 ± 2.5% (n = 14, mean ± SEM) of the current at 2 mM cGMP. At 32 μM cGMP, 10 μM tetracaine became much more effective, blocking essentially all of the current (Fig. 1 *A*, *right*). 32 μM cGMP activated only 22.6 ± 3.3% (n = 10) of the current seen at 2 mM cGMP. Tetracaine has an affinity for closed states of CNG channels that is approximately three orders of magnitude higher than for open states (Fodor et al., 1997). The greater block of 10 μM tetracaine at 32 μM cGMP is observed because the channels spent more time closed at 32 μM than at 2 mM cGMP.

We performed a similar experiment on channels in which the glutamic acid at position E363 had been mutated to a glycine, the residue normally present at a homologous position in the β subunit of the rod CNG channel (Chen et al., 1993). Fig. 1 *B* shows data collected from a patch in which 10 μM tetracaine had been applied to mutant E363G channels in the presence of either high (2 mM) or low (256 μM) concentrations of cGMP. Tetracaine block at 2 mM cGMP was less effective for E363G channels than it was for wild-type channels. At this saturating concentration of cGMP, 10 μM tetracaine blocked only 35.5 ± 3.5% (n = 11) of the current in E363G channels. Furthermore, tetracaine did not block E363G channels more effectively as more of the channels were closed at the lower concentration of cGMP. In E363G channels, 256 μM cGMP activated 46.2 ± 0.8% (n = 3) of the current seen at 2 mM cGMP. Yet, despite the fact that the channels were spending more time closed at 256 μM cGMP, 10 μM

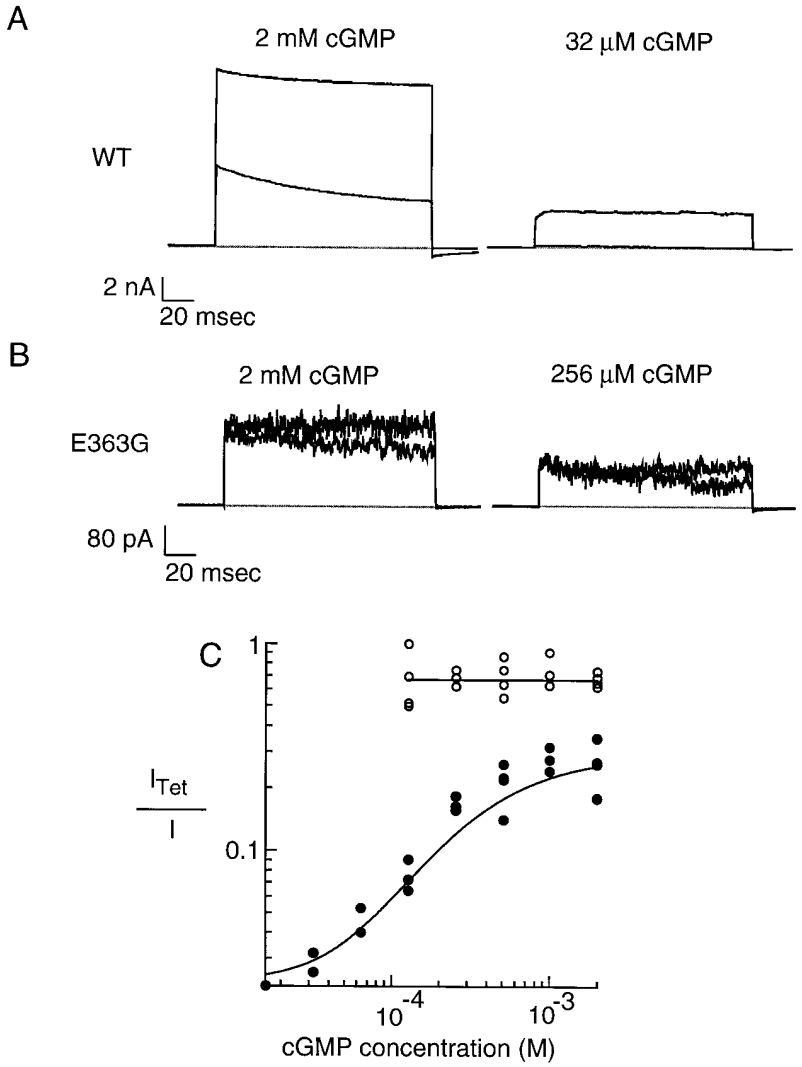

FIGURE 1. Tetracaine became more effective at low concentrations of cGMP for wild-type but not for E363G channels. (*A* and *B*) Comparison of the effect of 10 μM tetracaine on wild-type (*A*) and E363G (*B*) channels. Currents are in response to a voltage step to +60 mV from a holding potential of 0 mV. The currents recorded in the absence of tetracaine (*top traces*) are superimposed with the currents recorded in the presence of 10 μM tetracaine (*bottom traces*). Shaded lines show the zero current level. Leak current in the absence of cGMP has been subtracted from all traces. (*C*) The effect of 10 μM tetracaine at different concentrations of cGMP for wild-type rod channels (●, $n = 4$) or E363G channels (○, $n = 4$). Data pooled from a number of different patches. On the y-axis is the current, recorded with 10 μM tetracaine normalized by the current recorded in the absence of tetracaine at the concentration of cGMP indicated on the x-axis. All currents were measured at +60 mV. Fits to the data are from Scheme 1 (see text) with K = 4,500 M^{-1}, L = 17, K_{Dc} = 240 nM, K_{Do} = 180 μM for wild-type channels and $K_{Dc} = K_{Do}$ = 20 μM (i.e., no state dependence of tetracaine block) for E363G channels.

tetracaine blocked only 31.9 ± 4.3% ($n = 3$) of the current, indistinguishable from the block observed at saturating cGMP.

A simple allosteric model has previously been used (Fodor et al., 1997) to describe the state dependence of tetracaine block of wild-type CNG channels (Scheme 1).

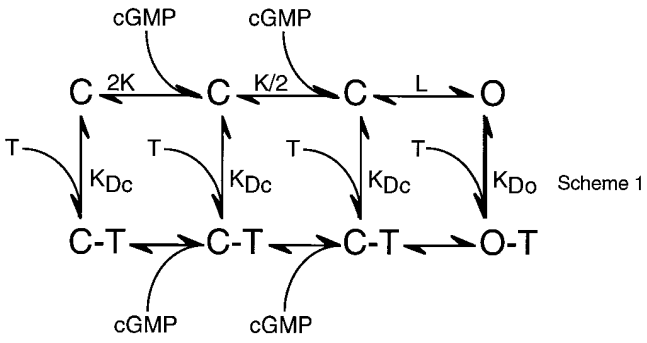

In this model, K is the equilibrium constant of the initial binding of cGMP to each subunit and L is the equilibrium constant of the allosteric transition from the fully liganded closed to the fully liganded open state. K_{Dc} is the disassociation constant of tetracaine from closed states of the channel and K_{Do} is the disassociation constant of tetracaine from the open state of the channel.

Fig. 1 *C* shows the effect of 10 μM tetracaine on wild-type (●) and E363G (○) channels at different concentrations of cGMP for a number of different patches as measured at +60 mV. Plotted on the y-axis is current in the presence of 10 μM tetracaine normalized by the current in the absence of tetracaine at the concentration of cGMP specified on the x-axis. For wild-type channels, the effectiveness of tetracaine as a blocker greatly increased as the cGMP concentration was lowered. The curve through the wild-type data is a fit of Scheme 1 with nearly three orders of magnitude higher binding affinity of tetracaine to closed states (K_{Dc} = 240 nM) than to the open state (K_{Do} = 180 μM). In contrast to wild-type channels, the effectiveness of tetracaine block did not change for E363G channels when the channels

spent more time in closed states at low cGMP concentrations (Fig. 1 *C*, ○).

One way to detect state-dependent block is to determine if the blocker produces a shift in the apparent affinity for cGMP. Fig. 2 compares the effect of 10 μM tetracaine on cGMP dose–response relations in wild-type (Fig. 2 *A*) and E363G (Fig. 2 *B*) channels as measured at +60 mV. The lines through the data show fits generated from the Hill equation of the form

$$\frac{I}{I_{\text{Max}}} = \frac{[\text{cGMP}]^n}{K_{1/2\,\text{cGMP}}^n + [\text{cGMP}]^n} \quad (1)$$

where I_{Max} is the current produced by saturating cGMP, n is the Hill slope (usually ~2 for these channels) and $K_{1/2\text{cGMP}}$ is the concentration of cGMP that produces half of the current seen at saturating cGMP. cGMP dose–response curves in the absence of tetracaine (Fig. 2, ●) were normalized by the current obtained at 2 mM cGMP. For comparison, cGMP dose–response curves in the presence of 10 μM tetracaine (Fig. 2, ○) were normalized by the current obtained in the presence of 2 mM cGMP and 10 μM tetracaine. In wild-type channels, tetracaine's state-dependent block caused the value of $K_{1/2\text{cGMP}}$ to shift from 70.7 ± 4.5 μM (n = 20) in the absence of tetracaine to 246.9 ± 13.8 μM (n = 4) in the presence of 10 μM tetracaine (Fig. 2 *A*). This shift in the apparent affinity for cGMP presumably occurred because tetracaine held the channels closed, and hence a higher concentration of cGMP was required to drive the channels into the open state (Fodor et al., 1997). The E363G mutation did not, as we have seen, eliminate tetracaine block of the channel, but it did eliminate the shift in apparent affinity for cGMP caused by 10 μM tetracaine. The normalized cGMP dose–response curves for E363G channels in the presence and absence of tetracaine are essentially identical (Fig. 2 *B*). The $K_{1/2\text{cGMP}}$ for E363G channels in the absence of tetracaine was 249.6 ± 24.6 μM (n = 10), very similar to the $K_{1/2\text{cGMP}}$ in the presence of 10 μM tetracaine, 280.6 ± 26.0 μM (n = 5). The elimination of the shift in the cGMP dose–response curve suggests that tetracaine binding is no longer state dependent in the mutant channel, and hence tetracaine no longer interferes with cGMP's ability to drive the channels into the open state.

Scheme 1 suggests that the fractional block seen in Fig. 1 *C* in the E363G channel would occur if the closed state affinity were 20 μM. For wild-type channels, the fit from the model gives a closed state affinity of 240 nM. The E363G mutation, therefore, reduced the affinity of tetracaine for the closed state by a factor of ~100. This result is consistent with the hypothesis that tetracaine's high affinity binding to closed states arises from an electrostatic interaction between the positively charged tetracaine molecule and the negatively charged glutamic acid. Alternatively, the effects seen in the E363G mutation may be due to the smaller side chain present in the glycine residue. In either case, tetracaine becomes a much less effective blocker of the E363G channel.

The E363G mutation eliminates Ni^{2+} relief of tetracaine block. E363G mutant channels have a significantly reduced apparent affinity for cGMP when compared with wild-type channels (Fig. 2), consistent with the hypothesis that the E363G mutation makes the opening transition less favorable. This hypothesis is in agreement with single-channel recordings that show that at room temperature and saturating concentrations of cGMP, the E363G channel is open <1% of the time (Sesti et al., 1996; Bucossi et al., 1997). This raises the possibility that the lack of state dependence observed in Fig. 1 *C* could be caused by most of the E363G channels being closed even at high concentrations of cGMP. If 99% of the E363G channels at saturating concentrations of cGMP were closed, then tetracaine's affinity for these closed channels would dominate tetracaine's affinity for the few open channels. If this were the case, there could be significant differences between tetracaine's

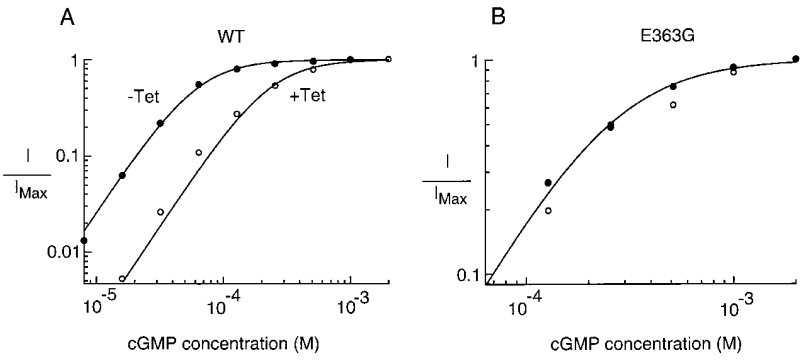

FIGURE 2. Tetracaine shifted the cGMP dose–response curve to the right in wild-type but not E363G channels. (*A* and *B*) cGMP dose–response curves in the absence and presence of 10 μM tetracaine for a patch containing wild-type (*A*) or E363G (*B*) channels. Currents in the absence of tetracaine are normalized to currents obtained in the presence of saturating (2 mM) cGMP. For comparison, currents in the presence of 10 μM tetracaine are normalized to currents obtained in the presence of saturating (2 mM) cGMP + 10 μM tetracaine. All currents were measured at +60 mV. Fits are to Eq. 1. For the wild-type rod channel in the absence of tetracaine: $K_{1/2\text{cGMP}}$ = 60.5 μM, n = 2.0. For the wild-type rod channel in the presence of 10 μM tetracaine, $K_{1/2\text{cGMP}}$ = 228 μM, n = 2.0. For the rod E363G channel both in the presence and absence of tetracaine, $K_{1/2\text{cGMP}}$ = 251 μM, n = 1.7.

ability to block the open and closed states that we would not detect as the remaining 1% of the channels closed at lower cGMP concentrations.

To address this possibility, we measured tetracaine affinity in the presence and absence of internal Ni^{2+}. Ni^{2+} has been shown to drive rod channels into the open state by making the opening transition more favorable. Ni^{2+} significantly potentiates currents recorded from the rod channel at low concentrations of cGMP (Ildefonse et al., 1992; Karpen et al., 1993; Gordon and Zagotta, 1995*a*) or at saturating concentrations of the partial ligand cAMP (Gordon and Zagotta, 1995*a*), conditions that cause the channel to spend significant periods of time in closed states. Fig. 3, *top* shows that, in agreement with previous results (Gordon and Zagotta, 1995*a*), application of 1 μM Ni^{2+} to wild-type channels caused essentially no increase in current when measured at +60 mV. A significant potentiation of current did not occur because wild-type channels at saturating cGMP are already open most of the time, so the increase in the favorability of the opening allosteric transition caused by Ni^{2+} cannot significantly increase the maximal current observed. Application of 10 μM Ni^{2+} to wild-type channels actually caused currents to decrease to 94.5 ± 2.0% (n = 5) of the current seen in the absence of Ni^{2+} (data not shown). This small decrease in current at 10 μM Ni^{2+} was caused by a small amount of Ni^{2+} block of the channels (Karpen et al., 1993; Gordon and Zagotta, 1995*a*).

In contrast to its effects on wild-type channels, Ni^{2+} produced substantial potentiation in E363G channels (Fig. 3, *bottom*). Application of 1 μM Ni^{2+} caused currents measured at +60 mV in the presence of saturating cGMP to increase by a factor of 2.76 ± 0.25 (n = 5), while 10 μM Ni^{2+} caused currents to increase by a factor of 3.11 ± 0.33 (n = 4). This robust potentiation by Ni^{2+} confirms that the E363G mutation caused a decrease in the open probability and that Ni^{2+} could increase the amount of time E363G channels spend open.

To test whether the E363G channel's low open probability could account for the apparent loss of state dependence of the block by tetracaine, we measured tetracaine dose–response curves in the presence of saturating concentrations of cGMP and 0, 1, or 10 μM internal Ni^{2+}. Fig. 4 *A* shows the effect of 10 μM Ni^{2+} on block of wild-type and E363G channels by 40 μM tetracaine. For wild-type channels in the absence of Ni^{2+}, 40 μM tetracaine blocked 89.8 ± 1.7% (n = 9) of the current. In the presence of 10 μM Ni^{2+}, however, 40 μM tetracaine became much less effective, blocking only 51.1 ± 2.0% (n = 3) of the current. Tetracaine presumably became less effective because Ni^{2+} increased the already high open probability of the channel. This small change in the open probability (e.g., from 0.96 to 0.98) is associated with a large change in the closed probability (e.g., from 0.04 to 0.02, a twofold change). Because tetracaine greatly prefers to bind to closed states, it is very sensitive to these changes in the fraction of time the channel spends closed (Fodor et al., 1997). Fig. 4 *B* shows tetracaine dose–response curves measured for wild-type channels in the absence (●), or presence of 1 (■) or 10 (▲) μM Ni^{2+}. As the Ni^{2+} con-

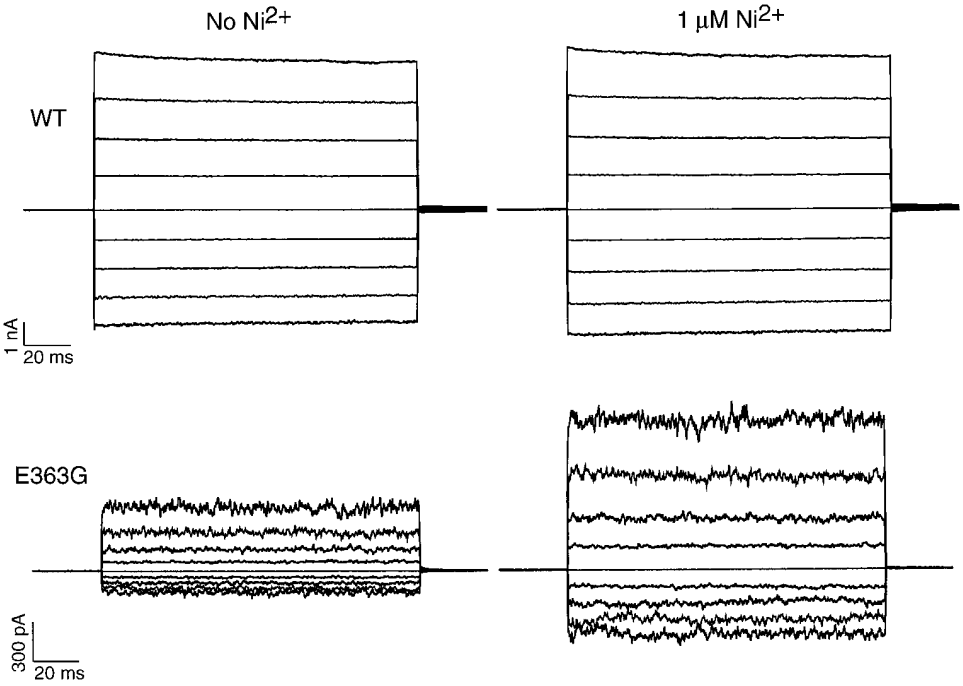

FIGURE 3. Ni^{2+} substantially increases the currents produced by saturating (4 mM) cGMP in E363G but not in wild-type channels. Currents are in response to families of voltage steps from a holding potential of 0 to between −80 and +80 mV in increments of +20 mV. Leak currents in the absence of cGMP have been subtracted.

centration increased, tetracaine became a less effective blocker and the tetracaine dose–response curve shifted to the right. In contrast, Ni^{2+} potentiation did not affect tetracaine apparent affinity for the E363G channel. Fig. 4 *C* shows that tetracaine dose–response curves for the E363G channel in the presence of saturating (2 mM) cGMP and 0 (●), 1 (■), and 10 (▲) μM Ni^{2+} were essentially identical. This is true despite the fact that Ni^{2+} robustly potentiates the E363G channels (Fig. 3).

The fits to the data in Fig. 4, *B* and *C* are the Hill equation in the form:

$$\frac{I_{\mathrm{Tet}}}{I} = \frac{K^n_{1/2\,\mathrm{Tet}}}{K^n_{1/2\,\mathrm{Tet}} + [\mathrm{Tet}]^n} \qquad (2)$$

where I is the current in the absence of tetracaine, I_{Tet} is the current in the presence of tetracaine, n is the Hill slope, and $K_{1/2\mathrm{Tet}}$ is the apparent affinity for tetracaine. Fig. 4 *D* shows values of $K_{1/2\mathrm{Tet}}$ derived from fits of this equation to tetracaine dose–response curves in the absence and presence of Ni^{2+}. In wild-type channels, increasing concentrations of Ni^{2+} made tetracaine less effective, increasing $K_{1/2\mathrm{Tet}}$. In contrast, tetracaine had essentially the same apparent affinity for the E363G channel at 0, 1, and 10 μM Ni^{2+}. These data suggest that the loss of cGMP dependence of tetracaine block seen for E363G channels in Fig. 1 is the result of a true loss of state dependence of tetracaine binding and not due merely to the lower open probability of mutant channels.

In addition to shifting the apparent affinity for tetracaine, the E363G mutation also shifted the Hill slope from 1 (Fodor et al., 1997) for wild-type channels to 1.20 ± 0.21 (n = 6) for E363G channels. While this is not a large difference, and was not enough to significantly affect the values of $K_{1/2\mathrm{Tet}}$ derived for E363G, most tetracaine dose–response curves for E363G were not well fit with a Hill slope of 1. We do not understand what caused this difference between wild-type and E363G channels.

Chimeric E363G channels with the olfactory NH_2 terminus also lack state-dependent block by tetracaine. Application of cytoplasmic Ni^{2+} is one way to increase the open probability of E363G channels. Another way is to substitute the NH_2 terminus of the olfactory channel into the rod channel (Goulding et al., 1994; Gordon and Zagotta, 1995*b*). The chimeric channel called CHM15, which has the olfactory NH_2 terminus substituted into the wild-type rod channel, has values for the equilibrium constant of the opening allosteric transition (L in Scheme 1) ~10-fold higher than wild-type rod channels (Gordon and Zagotta, 1995*b*). We reasoned that at saturating concentrations of cGMP the CHM15 channel with the E363G mutation would be open a higher fraction of the time than the rod channel with the E363G mutation. The improved open probability of CHM15-E363G channels would allow a better measurement of the effectiveness of tetracaine block on open channels with the E363G mutation. This in turn would further allow us to exclude the possibility that the lack of state de-

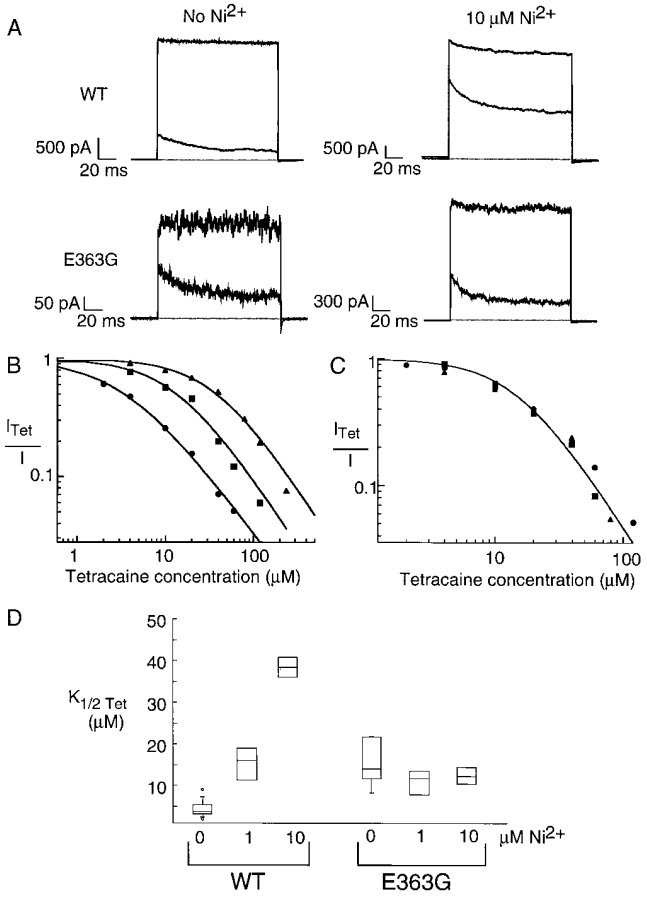

FIGURE 4. The E363G mutation eliminated Ni^{2+} relief of tetracaine block. (*A*) Block of wild-type and E363G channels in the absence and presence of Ni^{2+}. Currents are in response to a voltage step to +60 mV from a holding potential of 0 mV for four separate patches. In each panel, the top trace shows current in the absence of tetracaine and the bottom trace shows current in the presence of 40 μM tetracaine. The shaded line represents the zero current level. (*B*) Dose–response curves for tetracaine from three separate patches containing wild-type rod channels in the presence of 0 (●), 1 (■), and 10 (▲) μM Ni^{2+}. All currents were measured at +60 mV. All currents were recorded in the presence of saturating (2 mM) cGMP and normalized by currents recorded in the absence of tetracaine. Fits are to Eq. 2. For 0 μM Ni^{2+}: $K_{1/2\mathrm{Tet}}$ = 3.4 μM, n = 1.0; for 1 μM Ni^{2+}: $K_{1/2\mathrm{Tet}}$ = 13.3 μM, n = 1.1; and for 10 μM Ni^{2+}: $K_{1/2\mathrm{Tet}}$ = 37.7 μM, n = 1.0. (*C*) Dose–response curves for tetracaine for three separate patches recorded from E363G channels in the presence of 0 (●), 1 (■), and 10 (▲) μM Ni^{2+}. The fit is to Eq. 2 with $K_{1/2\mathrm{Tet}}$ = 15.19 μM, n = 1.6. (*D*) Box plots showing range of tetracaine apparent affinities for wild-type and E363G channels in 0, 1, and 10 μM Ni^{2+}. The line in the middle of the boxes shows the median. The top and bottom edges of the boxes show the 25th and 75th percentiles of the data. The whiskers coming out of some of the boxes show the 5th and 95th percentiles. Circles represent outliers.

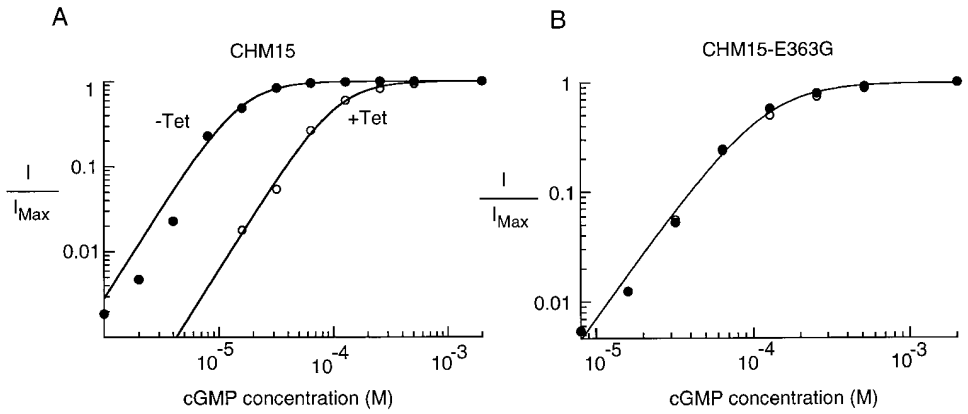

FIGURE 5. Tetracaine shifted the cGMP dose–response curve to the right in CHM15 but not CHM15-E363G channels. (*A* and *B*) cGMP dose–response curves in the absence and presence of 40 μM tetracaine for a patch containing CHM15 (*A*) or CHM15-E363G (*B*) channels. Currents in the absence of tetracaine are normalized by currents obtained in the presence of saturating (2 mM) cGMP. For comparison, currents in the presence of 40 μM tetracaine are normalized by currents obtained in the presence of saturating (2 mM) cGMP + 40 μM tetracaine. All currents were measured at +60 mV. Fits are to Eq. 1. For the CHM15 channel in the absence of tetracaine, $K_{1/2cGMP}$ = 15.6 μM, n = 2.1. For the CHM15 channel in the presence of 40 μM tetracaine, $K_{1/2cGMP}$ = 108.7 μM, n = 2.1. And for the CHM15-E363G channel both in the presence and absence of tetracaine, $K_{1/2cGMP}$ = 117.0 μM, n = 2.0.

pendence observed in E363G channels was due to the low open probability of these channels, causing us to miss tetracaine's behavior on the few open channels.

As expected, substitution of the olfactory channel's NH_2 terminus shifted the apparent affinity for cGMP from 249.6 ± 24.6 μM (n = 10) in the rod channel with the E363G mutation to 119.2 ± 9.1 μM (n = 5) in the CHM15-E363G channel. This confirms that the presence of the olfactory NH_2 terminus produces E363G channels in which the opening allosteric transition is more favorable.

Fig. 5 compares cGMP dose–response curves in the absence (●) and presence (○) of 40 μM tetracaine for CHM15 (Fig. 5 *A*) and CHM15-E363G (Fig. 5 *B*). As was the case for wild-type channels (Fig. 2 *A*), application of tetracaine to CHM15 caused a substantial shift in the values for $K_{1/2cGMP}$ from 20.6 ± 2.1 μM (n = 10) in the absence to 125.4 ± 14.4 μM (n = 5) in the presence of 40 μM tetracaine (Fig. 5 *A*). In the CHM15-E363G channel, this shift in the cGMP dose–response curve was eliminated (Fig. 5 *B*). The $K_{1/2cGMP}$ for E363G channels in the presence of 40 μM tetracaine, 116.6 ± 1.0 μM (n = 3), was essentially identical to the $K_{1/2cGMP}$ in the absence of tetracaine, 119.2 ± 9.1 μM (n = 5).

Fig. 6 *A* compares 40 μM tetracaine block at a high (2 mM) and low (32 μM) concentration of cGMP for a patch containing CHM15 channels. As was the case for wild-type rod channels, lowering cGMP concentration caused tetracaine to become much more effective. Fig. 6 *B* shows a similar experiment comparing 40 μM tetracaine block at a high (2 mM) and low (128 μM) concentration of cGMP for a patch containing CHM15-E363G channels. As was the case for E363G channels, tetracaine block did not become more effective as more of the CHM15-E363G channels were closed at the lower cGMP concentration. Fig. 6 *C* compares fractional block of 40 μM tetracaine measured at +60 mV for CHM15 and CHM15-E363G channels from a number of patches

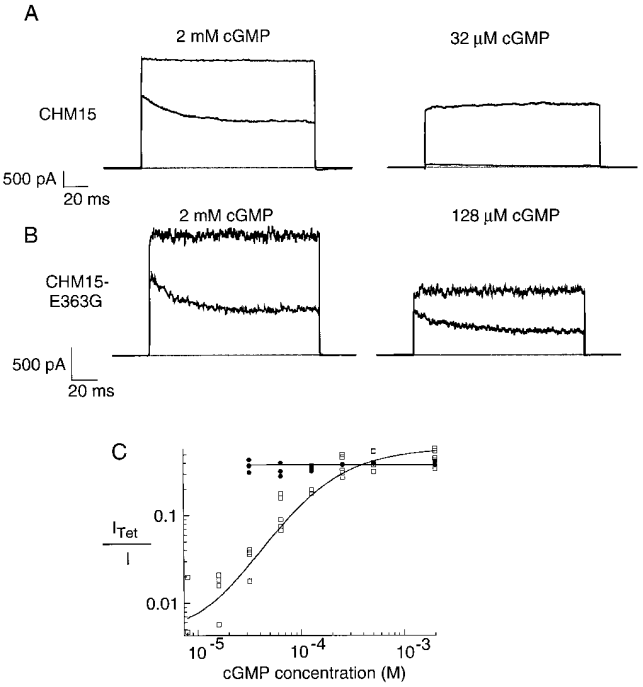

FIGURE 6. Tetracaine becomes more effective at low concentrations of cGMP for CHM15 but not for CHM15-E363G channels. (*A* and *B*) Comparison of the effect of 40 μM tetracaine on CHM15 (*A*) and CHM15-E363G (*B*) channels. Currents are in response to a voltage step to +60 mV from a holding potential of 0 mV. The currents recorded in the absence of tetracaine (*top traces*) are superimposed with the currents recorded in the presence of 40 μM tetracaine (*bottom traces*). Shaded lines show the zero current level. Leak current in the absence of cGMP has been subtracted from all traces. (*C*) The effect of 40 μM tetracaine at different concentrations of cGMP for CHM15 (□, n = 5) or CHM15-E363G (●, n = 4) channels. Data were pooled from a number of different patches. On the y-axis is the current, recorded with 40 μM tetracaine normalized by the current recorded in the absence of tetracaine at the concentration of cGMP indicated on the x-axis. All currents were measured at +60 mV. Fits to the data are from Scheme 1, with K = 4,500 M^{-1}, L = 300, K_{Dc} = 200 nM, K_{Do} = 200 μM for CHM15 channels and K_{Dc} = K_{Do} = 25 μM (i.e., no state dependence of tetracaine block) for CHM15-E363G channels.

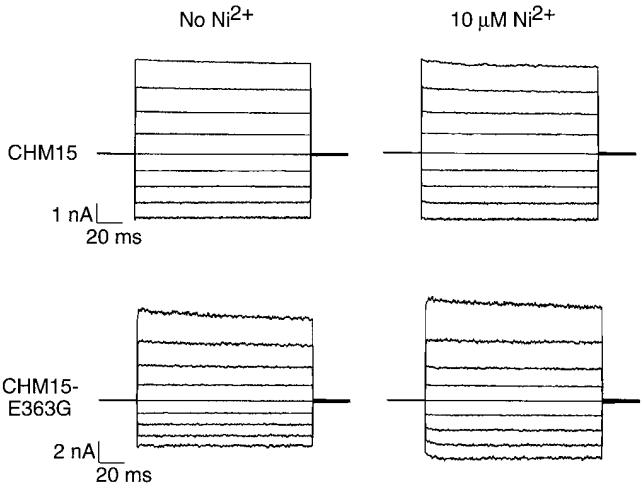

FIGURE 7. The effects of Ni^{2+} on CHM15 and CHM15-E363G. Currents are in response to families of voltage steps from a holding potential of 0 to between −80 and +80 mV in increments of +20 mV. Leak currents in the absence of cGMP have been subtracted.

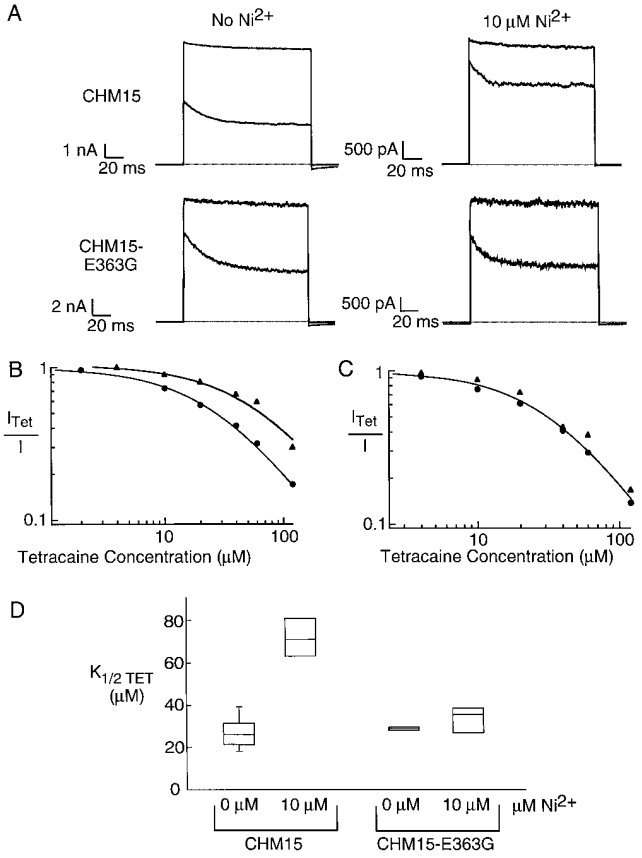

FIGURE 8. The E363G mutation in CHM15 eliminated Ni^{2+} relief of tetracaine block. (*A*) Block of CHM15 and CHM15-E363G channels in the absence and presence of Ni^{2+}. Currents are in response to a voltage step to +60 mV from a holding potential of 0 mV for four separate patches. In each panel, the top trace shows current in the absence of tetracaine and the bottom trace shows current in the presence of 40 μM tetracaine. The shaded line represents the zero current level. (*B*) Dose–response curves for tetracaine from two separate patches containing CHM15 channels in the presence of 0 (●) or 10 (▲) μM Ni^{2+}. All currents were measured at +60 mV. All currents were recorded in the presence of saturating (2 mM) cGMP and normalized by currents recorded in the absence of tetracaine. Fits are to Eq. 2. For 0 μM Ni^{2+}: $K_{1/2Tet}$ = 26.5 μM, n = 1.0; for 10 μM Ni^{2+}: $K_{1/2Tet}$ = 59.4 μM, n = 1.0. (*C*) Dose–response curves for tetracaine for two separate patches recorded from CHM15-E363G channels in the presence of 0 (●) or 10 (▲) μM Ni^{2+}. The fit is to Eq. 2 with $K_{1/2Tet}$ = 31.0 μM, n = 1.3. (*D*) Box plot showing range of tetracaine-apparent affinities for CHM15 and CHM15-E363G channels in 0 and 10 μM Ni^{2+}. The line in the middle of the boxes shows the median. The top and bottom edges of the boxes show the 25th and 75th percentiles of the data. The whiskers coming out of some of the boxes show the 5th and 95th percentiles.

over a range of cGMP concentrations. As was the case for wild-type channels (Fig. 1), decreasing cGMP concentration caused tetracaine block to increase for CHM15 channels, and this relationship was well described by Scheme 1. Lowering cGMP concentration, however, did not change the degree of tetracaine block of CHM15-E363G channels.

The CHM15-E363G channel contains H420 from the rod channel, which allows for Ni^{2+} potentiation (Gordon and Zagotta, 1995*b*). We exploited the presence of this potentiating histidine to drive these channels further into the open state by applying Ni^{2+}. Application of 10 μM Ni^{2+} confirmed that the CHM15-E363G channel (Fig. 7) spends considerably more time in the open state than does the E363G channel with the rod NH_2 terminus. When measured at +60 mV, CHM15-E363G currents in the presence of Ni^{2+} were identical to those measured in the absence of Ni^{2+} ($I_{Ni^{2+}}/I = 1.0 \pm 0.1$, $n = 3$). This is in contrast to the E363G mutation in the rod channel, where application of Ni^{2+} caused the current to increase (Fig. 3). As was the case for wild-type channels, application of 10 μM Ni^{2+} caused a slight block of the CHM15 channel ($I_{Ni^{2+}}/I = 0.94 \pm 0.013$, $n = 3$).

We measured tetracaine dose–response curves for CHM15 and CHM15-E363G channels in the presence of saturating concentrations of cGMP and 10 μM internal Ni^{2+}. Fig. 8 *A* shows the effects of 10 μM Ni^{2+} on 40 μM tetracaine block of currents in CHM15 and CHM15-E363G channels. Ni^{2+} decreased tetracaine's effectiveness on CHM15 channels, but not CHM15-E363G channels. Application of 10 μM Ni^{2+} to the CHM15 channel shifted tetracaine's dose–response curve to the right (Fig. 8 *B*) while not changing tetracaine's dose–response curve for the CHM15-E363G channel (Fig. 8 *C*). Fig. 8 *D* shows a box plot comparing values of $K_{1/2Tet}$ measured at +60 mV for CHM15 and CHM15-E363G channels in the presence and absence of Ni^{2+}. Application of 10 μM Ni^{2+} changed the apparent affinity of tetracaine for CHM15. For CHM15-E363G, however, the apparent affinity of tetracaine in the presence of 10 μM

Ni^{2+} was essentially indistinguishable from the apparent affinity in the absence of Ni^{2+}.

Taken together, these results show that even in the wider range of open probabilities obtained in the presence of the olfactory amino terminus, we were unable to detect any state dependence to tetracaine block in the presence of the E363G mutation. These results strongly support our hypothesis that the state dependence of tetracaine binding arises from a conformational change that occurs at the E363 residue.

DISCUSSION

Tetracaine block of wild-type rod and olfactory CNG channels displays strong state dependence, with the affinity for closed channels approximately three orders of magnitude higher than the affinity for open channels (Fodor et al., 1997). In wild-type channels, tetracaine became more effective as channels spent more time closed at lower cGMP concentrations and less effective as channels were driven into open states with high concentrations of cGMP and internal Ni^{2+}. We have shown that the pore mutation E363G eliminated the state dependence of tetracaine block. Tetracaine was equally effective at blocking E363G channels at low concentrations of cGMP or at high concentrations of cGMP and internal Ni^{2+}. Similar results were obtained on channels in which the olfactory NH_2 terminus had been introduced into the rod channel. These chimeric channels had a higher value for the equilibrium constant of the opening allosteric transition than their rod counterparts. This allowed tetracaine block to be studied over a broader range of open probabilities.

A model that is consistent with our results is shown in Fig. 9. This model envisions strong, stabilizing electrostatic interactions between tetracaine's positive charge and the negative charge of E363 in the closed state of the wild-type channel. This electrostatic interaction confers tetracaine's high affinity binding to the closed states of CNG channels. The conformational change in the pore that accompanies channel opening moves E363 away from tetracaine's positive charge. This movement of E363 during channel opening significantly weakens tetracaine's ability to bind to the open pore. Alternatively, it is possible that the opening conformational change might prevent access of tetracaine to E363. The state dependence of tetracaine block observed in wild-type channels, therefore, arises from tetracaine's ability to interact with E363 in the closed, but not the open, conformations of the pore. Neutralization of this charge via the E363G mutation specifically eliminates tetracaine's high affinity binding to closed states of the channel and hence eliminates the state dependence of tetracaine block.

The model in Fig. 9 argues that in the closed conformation of the pore, E363G is accessible to internally applied tetracaine. The E363 residue has previously been

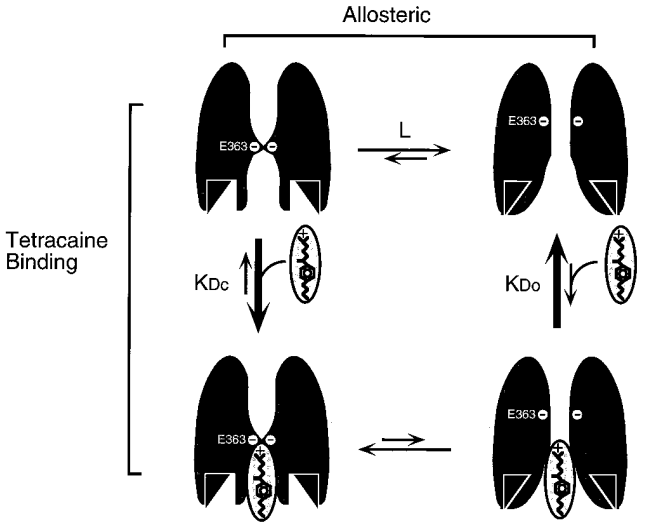

FIGURE 9. State-dependent tetracaine block in wild-type channels. See text.

shown to be part of the site that binds externally applied monovalent and divalent cations (Root and MacKinnon, 1993; Eismann et al., 1994; Sesti et al., 1995). Mutations at the E363 position, however, still leave the channel vulnerable to block by internal divalent cations, suggesting that there is a second, internal cation binding site. The specific residues that contribute to this internal binding site remain unknown. Sun et al. (1996) used cysteine-scanning mutagenesis to examine which regions of the pore were accessible to internally and externally applied cysteine-modifying reagents. The E363C mutation did not produce functional channels, but the residues immediately adjacent to E363 were both accessible from both the inside and the outside of the channel. This suggests that E363 is in a region of the pore that can be accessed from both sides of the membrane. The state dependence of tetracaine binding suggests that E363 may be more accessible from the inside when the channel is closed.

Mutations at the E363 position produce in the channel nonconducting states that are not included in our simple model of tetracaine block (Bucossi et al., 1996). The existence of these nonconducting states, however, is unlikely to explain the phenomena that we have observed in this paper. If these states had a high affinity for tetracaine, then tetracaine should have become more effective for the E363G mutation than for wild-type channels. Clearly, this did not happen. If these states had a very low affinity for tetracaine, and the vast majority of the channels in a patch were in this state, then it is possible that the state dependence of the remaining channels would be overwhelmed by the nonconducting state. For the state dependence of the remaining channels to be undetectable, however, we estimate that 95–98% of the channels in a patch would

have to be in this nonconducting state. This seems unlikely, especially in the CHM15 background where robust currents were common.

The negative charge at E363 is well conserved throughout the superfamily of voltage-gated channels (Heginbotham et al., 1992). Local anesthetics block many members of this superfamily with sometimes quite complex state dependence. This raises the possibility that the interaction described in this paper may influence the state dependence of a wide range of drug–receptor interactions. Future research using different combinations of channels and drugs may shed light on the pervasiveness of this interaction and provide a higher resolution picture of how E363 moves in relationship to other residues in the pore during the opening of CNG and voltage-gated channels.

We thank R.R. Reed for the rat olfactory cDNA clone and E.R. Liman for the high expression vector. In addition, we thank Gay Sheridan and Heidi Utsugi for technical assistance and Galen Eaholtz, Sharona Gordon, Bertil Hille, Mark Shapiro, and Elizabeth Sunderman for comments on the manuscript.

This work was supported by a grant from the National Eye Institute (EY 10329 to W.N. Zagotta) and the Human Frontiers Science Program. W.N. Zagotta is an Investigator of the Howard Hughes Medical Institute.

Original version received 6 June 1997 and accepted version received 11 August 1997.

REFERENCES

Bucossi, G., E. Eismann, F. Sesti, M. Nizzari, M. Seri, U.B. Kaupp, and V. Torre. 1996. Time-dependent current decline in cyclic GMP-gated bovine channels caused by point mutations in the pore region expressed in Xenopus oocytes. *J. Physiol. (Camb.).* 493:409–418.

Bucossi, G., M. Nizzari, and V. Torre. 1997. Single-channel properties of ionic channels gated by cyclic nucleotides. *Biophys. J.* 72: 1165–1181.

Chen, T.Y., Y.W. Peng, R.S. Dhallan, B. Ahamed, R.R. Reed, and K.W. Yau. 1993. A new subunit of the cyclic nucleotide-gated cation channel in retinal rods. *Nature (Lond.).* 362:764–767.

Eismann, E., F. Muller, S.H. Heinemann, and U.B. Kaupp. 1994. A single negative charge within the pore region of a cGMP-gated channel controls rectification, Ca2+ blockage, and ionic selectivity. *Proc. Natl. Acad. Sci. USA.* 91:1109–1113.

Fodor, A.A., S.E. Gordon, and W.N. Zagotta. 1997. Mechanisms of tetracaine block of cyclic nucleotide–gated channels. *J. Gen. Physiol.* 109:3–14.

Furman, R.E., and J.C. Tanaka. 1990. Monovalent selectivity of the cyclic guanosine monophosphate-activated ion channel. *J. Gen. Physiol.* 96:57–82.

Gordon, S.E., and W.N. Zagotta. 1995*a*. A histidine residue associated with the gate of the cyclic nucleotide–activated channels in rod photoreceptors. *Neuron.* 14:177–183.

Gordon, S.E., and W.N. Zagotta. 1995*b*. Localization of regions affecting an allosteric transition in cyclic nucleotide–activated channels. *Neuron.* 14:857–864.

Goulding, E.H., G.R. Tibbs, and S.A. Siegelbaum. 1994. Molecular mechanism of cyclic-nucleotide–gated channel activation. *Nature (Lond.).* 372:369–374.

Haynes, L.W. 1992. Block of the cyclic GMP-gated channel of vertebrate rod and cone photoreceptors by l-*cis*-diltiazem. *J. Gen. Physiol.* 100:783–801.

Heginbotham, L., T. Abramson, and R. MacKinnon. 1992. A functional connection between the pores of distantly related ion channels as revealed by mutant K+ channels. *Science (Wash. DC).* 258:1152–1155.

Hille, B. 1992. Ionic Channels of Excitable Membranes. Sinauer Associates Inc., Sunderland, MA.

Ildefonse, M., S. Crouzy, and N. Bennett. 1992. Gating of retinal rod cation channel by different nucleotides: comparative study of unitary currents. *J. Membr. Biol.* 130:91–104.

Jan, L.Y., and Y.N. Jan. 1990. A superfamily of ion channels. *Nature (Lond.).* 345:672.

Karpen, J.W., R.L. Brown, L. Stryer, and D.A. Baylor. 1993. Interactions between divalent cations and the gating machinery of cyclic GMP–activated channels in salamander retinal rods. *J. Gen. Physiol.* 101:1–25.

Kaupp, U.B., T. Niidome, T. Tanabe, S. Terada, W. Bonigk, W. Stuhmer, N.J. Cook, K. Kangawa, H. Matsuo, T. Hirose, et al. 1989. Primary structure and functional expression from complementary DNA of the rod photoreceptor cyclic GMP-gated channel. *Nature (Lond.).* 342:762–766.

Lancet, D. 1986. Vertebrate olfactory reception. *Annu. Rev. Neurosci.* 9:329–355.

McLatchie, L.M., and H.R. Matthews. 1992. Voltage-dependent block by L-cis-diltiazem of the cyclic GMP–activated conductance of salamander rods. *Proc. R. Soc. Lond. B Biol. Sci.* 247:113–119.

McLatchie, L.M., and H.R. Matthews. 1994. The effect of pH on the block by L-cis-diltiazem and amiloride of the cyclic GMP–activated conductance of salamander rods. *Proc. R. Soc. Lond. B Biol. Sci.* 255:231–236.

Root, M.J., and R. MacKinnon. 1993. Identification of an external divalent cation-binding site in the pore of a cGMP-activated channel. *Neuron.* 11:459–466.

Root, M.J., and R. MacKinnon. 1994. Two identical noninteracting sites in an ion channel revealed by proton transfer. *Science (Wash. DC).* 265:1852–1856.

Sesti, F., U.B. Kaupp, E. Eismann, M. Nizzari, and V. Torre. 1995. The multi-ion nature of the cGMP-gated channel from vertebrate rods. *J. Physiol.* (Camb.). 487:17–36.

Sesti, F., M. Nizzari, and V. Torre. 1996. Effect of changing temperature on the ionic permeation through the cyclic GMP–gated channel from vertebrate photoreceptors. *Biophys. J.* 70:2616–2639.

Sun, Z.P., M.H. Akabas, E.H. Goulding, A. Karlin, and S.A. Siegelbaum. 1996. Exposure of residues in the cyclic nucleotide–gated channel pore: *P* region structure and function in gating. *Neuron.* 16:141–149.

Yau, K.W., and D.A. Baylor. 1989. Cyclic GMP–activated conductance of retinal photoreceptor cells. *Annu. Rev. Neurosci.* 12:289–327.

Zimmerman, A.L., J.W. Karpen, and D.A. Baylor. 1988. Hindered diffusion in excised membrane patches from retinal rod outer segments. *Biophys. J.* 54:351–355.

Zufall, F., S. Firestein, and G.M. Shepherd. 1994. Cyclic nucleotide–gated ion channels and sensory transduction in olfactory receptor neurons. *Annu. Rev. Biophys. Biomol. Struct.* 23:577–607.